


## Recoil-limited feedback cooling of single nanoparticles near the ground state in an optical lattice

M. Kamba, H. Kiuchi, T. Yotsuya, and K. Aikawa

*Department of Physics, Tokyo Institute of Technology, Ookayama 2-12-1, Meguro-ku 152-8550 Tokyo*

 (Received 24 November 2020; revised 26 January 2021; accepted 12 May 2021; published 27 May 2021)

We report on direct feedback cooling of single nanoparticles in an optical lattice to near their motional ground state. We find that the laser phase noise triggers severe heating of nanoparticles' motion along the optical lattice. When the laser phase noise is decreased by orders of magnitude, the heating rate is reduced and accordingly the occupation number is lowered to about 3. We establish a model directly connecting the heating rate and the measured laser phase noise and elucidate that the occupation number under the lowest laser phase noise in our system is limited only by photon recoil heating. Our results show that the reduction of the laser phase noise near the oscillation frequency of nanoparticles is crucial for bringing them near the ground state and pave the way to sensitive accelerometers and quantum mechanical experiments with ultracold nanoparticles in an optical lattice.

DOI: [10.1103/PhysRevA.103.L051701](https://doi.org/10.1103/PhysRevA.103.L051701)

*Introduction.* Decelerating the motion of microscopic particles such as atoms and molecules has been an essential ingredient for revealing their fundamental properties and for realizing their applications in various fields, ranging from precision measurements [1,2] and fundamental physics [3] to quantum information processing [4,5] and quantum simulations [6,7]. In comparison with microscopic particles, decelerating the motion of mesoscopic and macroscopic particles has been a challenging task because of the lack of the efficient mechanism for deceleration. Nanometer-sized objects prepared near their motional ground state are expected to be a promising system for various applications including force sensing [8–10], the test of superposition states at macroscopic scales [11,12], detecting gravitational waves at high frequencies [13], and the search for non-Newtonian gravity forces [14].

In recent years, remarkable progress has been made in decelerating the motion of nanoparticles in vacuum either by feedback cooling or by cavity cooling. In the former scheme, a time-varying force opposite to the velocity of particles is applied [15–20], whereas the latter scheme relies on photon scattering in a high-finesse cavity transferring the motional energy of particles to photons [21–24]. Very recently, these approaches have been applied for cooling nanoparticles in a single-beam optical trap to near their motional ground state [25,26]. Aside from a single-beam optical trap, an optical lattice, a standing wave potential created by retroreflecting a laser, has been a crucial tool for trapping and manipulating atoms and molecules [6,7]. However, in spite of its possibility in diverse quantum mechanical experiments thanks to the high oscillation frequency in an optical lattice, the use of an optical lattice for nanoparticles has been limited [8,18,27].

In this Letter, we show that single charged nanoparticles trapped in an optical lattice are brought to near their ground state along the optical lattice at an ambient temperature via electric feedback cooling, namely, cold damping [18–20,28–31]. To make the impact of the laser phase noise (LPN) negligible, we minimize the distance of the trap from the retroreflecting mirror and also stabilize the laser frequency to an

optical resonator. We establish a model directly connecting the independently measured LPN and the heating rate of nanoparticles' motion and find that the heating rate increases as the LPN increases. Our model shows that the LPN near the oscillation frequency plays a crucial role in the heating dynamics. Furthermore, in our setup, the impact of the LPN is negligible and the residual heating mechanism limiting the lowest attainable occupation number is random photon scattering of the trapping laser. Our results are also useful in other fields involving an optical lattice, such as cold atoms and molecules, for evaluating the impact of the LPN on trapped particles.

*Theoretical model.* We start our discussions by introducing a theoretical model for the motion of nanoparticles in an optical lattice driven by the LPN on the basis of previous studies [18,19,32]. We describe the one-dimensional motion of nanoparticles along the optical lattice in the presence of fluctuating forces and damping mechanisms,

$$\ddot{q} + \Gamma_{\text{tot}}\dot{q} + \Gamma_c\dot{q}_n + \Omega_z^2(q + P_n) = \frac{F_{\text{BG}} + F_r}{m}, \quad (1)$$

with  $\Gamma_{\text{tot}} = \Gamma_{\text{BG}} + \Gamma_c + \Gamma_r + \Gamma_p$ . Here  $q$  and  $q_n$  denote the position of nanoparticles and the noise in the feedback signal, respectively, while  $\Gamma_{\text{BG}}$ ,  $\Gamma_c$ ,  $\Gamma_r$ , and  $\Gamma_p$  denote the damping rate due to collisions with background gases, the damping rate due to feedback cooling, the damping rate due to photon recoils, and the damping rate due to the LPN, respectively. In addition,  $m$ ,  $\Omega_z$ ,  $P_n$ ,  $F_{\text{BG}}$ , and  $F_r$  denote the mass of trapped nanoparticles, the oscillation frequency along the optical lattice, the stochastic force from the LPN, the stochastic force from background gases, and the stochastic force from photon scattering, respectively [33].  $T_{\text{eff}}$  for the particle following Eq. (1) is given as

$$T_{\text{eff}} = T_0 \frac{\Gamma_{\text{BG}}}{\Gamma_{\text{tot}}} + \frac{m\Omega_z^2 S_n \Gamma_c^2}{2k_B \Gamma_{\text{tot}}} + \frac{\hbar\omega_0 P_{\text{sc}}}{5mc^2 k_B \Gamma_{\text{tot}}} + \frac{m\Omega_z^6}{k_B} I(\Gamma_{\text{tot}}),$$

$$I(\Gamma_{\text{tot}}) = \frac{1}{2\pi} \int_{-\infty}^{\infty} \frac{\tilde{P}_n^2(\omega) d\omega}{(\Omega_z^2 - \omega^2)^2 + \omega^2 \Gamma_{\text{tot}}^2}, \quad (2)$$

where  $T_0$ ,  $S_n$ ,  $\omega_0$ ,  $P_{sc}$ ,  $c$ , and  $\tilde{P}_n(\omega)$  are the temperature of background gases, the power spectral density (PSD) of  $q_n$ , the frequency of the trapping light, the optical power scattered by nanoparticles, the speed of light, and the Fourier transform of  $P_n$ , respectively. The stochastic forces  $F_{BG}$  and  $F_r$  in Eq. (1) are characterized by  $T_0$  and  $P_{sc}$ , respectively.  $\tilde{P}_n(\omega)$  is obtained by multiplying  $\lambda d/c$  by the PSD of the LPN.

In general, the integral of Eq. (2) has to be numerically evaluated. However, considering that the spectral width of the integrand  $\Gamma_{tot}$  is much smaller than  $\Omega_z$ , to a good approximation we can write the integral as

$$I(\Gamma_{tot}) = \frac{\tilde{P}_n^2(\Omega_z)}{2\Omega_z^2\Gamma_{tot}}. \quad (3)$$

We confirm that this approximation does not deviate from the numerically obtained values by more than 2% with  $\Gamma_{tot} < 2\pi \times 300$  Hz, which is satisfied for the measurement of  $\gamma_{tot}$  [33].

At low pressures, in the absence of feedback cooling, the heating rate  $\gamma_{tot}$  is obtained from  $\Gamma_r$  and  $\Gamma_p$  as  $\gamma_{tot} = \gamma_p + \gamma_r$ , with  $\gamma_p = E_p\Gamma_p$  and  $\gamma_r = E_r\Gamma_r$ , where  $E_r$  and  $E_p$  denote the energies of nanoparticles at equilibrium for photon recoil heating and for LPN heating, respectively.  $E_r$  and  $E_p$  are approximately given by the photon energy  $\hbar\omega_0$  and the potential depth, respectively. The former is of the order of  $k_B \times 10^4$  K, while the latter is of the order of  $k_B \times 10^5$  K (see later discussions on our experiments). Since  $\gamma_{tot}$  is directly connected to the equilibrium occupation number as [32]

$$n_{eq} + \frac{1}{2} = \frac{\gamma_{tot}}{\hbar\Omega_z\Gamma_{tot}}, \quad (4)$$

we obtain the expression for  $\gamma_{tot}$  as follows by comparing Eqs. (2), (3), and (4):

$$\gamma_{tot} = \frac{1}{2}m\Omega_z^4\tilde{P}_n^2(\Omega_z) + \frac{\hbar\omega_0 P_{sc}}{5mc^2}. \quad (5)$$

The occupation number in the presence of feedback cooling at low pressures  $n_{eq}$  is then written as

$$n_{eq} + \frac{1}{2} = \frac{1}{2\Gamma_c\hbar\Omega_z} [2\gamma_{tot} + m\Omega_z^2 S_n \Gamma_c^2]. \quad (6)$$

In this model, the feedback gain is represented by  $\Gamma_c$  determined by the amplitude of the applied electric field [18]. While the first term of Eq. (6) is decreased by increasing  $\Gamma_c$ , the second term representing heating driven via the feedback loop increases with  $\Gamma_c$ . Thus,  $n_{eq}$  is minimized to  $\sqrt{2\gamma_{tot}mS_n/\hbar} - 1/2$  at an optimum feedback gain.

*Experiments.* In our experiments, we trap silica nanoparticles with radii of about  $R = 220$  nm in a one-dimensional optical lattice formed with a fiber laser [Fig. 1(a)] [18,27,34]. The radii of nanoparticles in the present work are several times larger than typical values in previous studies [15–17,19,20,25,26]. We load nanoparticles into the optical lattice at around 600 Pa by blowing up silica powders with a pulsed laser, similarly to light-induced desorption of nanoparticles attached on a surface [22,35]. After we load nanoparticles in one of lattice sites, we sweep the laser frequency and adjust their position to the focus of the incident beam where  $\Omega_z$  takes a maximum value. For a typical exper-

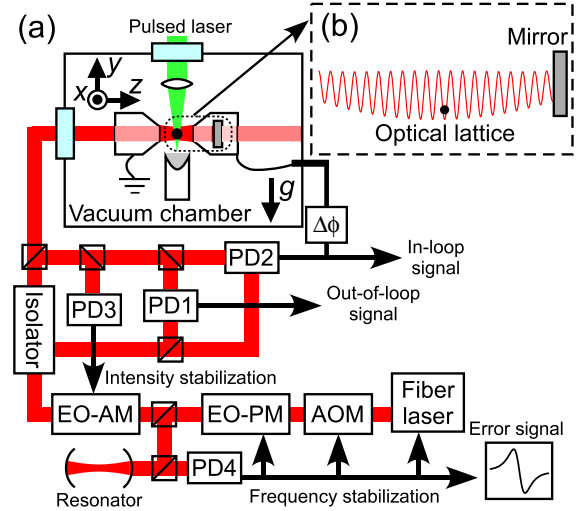


FIG. 1. (a) Schematic representation of our experimental setup. Single nanoparticles are trapped in an optical lattice formed by a single-frequency fiber laser at  $\lambda = 1550$  nm, which is intensity stabilized by an electro-optic amplitude modulator (EO-AM) and frequency stabilized by an electro-optic phase modulator (EO-PM) and an acousto-optic modulator (AOM). The motion of nanoparticles is observed via photodetectors (PDs). (b) Blow up near the trapping region. Nanoparticles are located at the focus of the incident beam where the oscillation frequency along the optical lattice is the highest. The position fluctuation of nanoparticles due to fluctuations in the laser frequency scales linearly with the distance from the retroreflecting mirror.

imental condition with a laser power of 168 mW,  $\Omega_z/2\pi$  is about 200 kHz, while the oscillation frequencies perpendicular to the light propagation direction are 64 and 73 kHz in the  $x$  and  $y$  directions, respectively [Fig. 2(b)]. The trapped nanoparticles experience a potential depth of  $5 \times 10^5$  K.

We observe the three-dimensional motion of nanoparticles with two photodetectors measuring the spatiotemporal variation of the infrared light scattered by them [17], where one of the detectors is used as an in-loop (IL) detector for feedback cooling and the other is used as an out-of-loop (OL) detector for measuring the motional temperatures  $T_{eff}$  [16,17,19].  $T_{eff}$  is obtained by comparing the integrated area of the PSDs of nanoparticles with and without cooling [16,17]. The PSD without cooling is obtained at around 10 Pa where the influence of laser absorption is negligible [33,36]. Using the measured position information, we realize three-dimensional electric feedback cooling of charged nanoparticles by applying three-dimensional electric fields synchronized to their motion such that their motional amplitudes are attenuated in all directions [18].

TABLE I. Experimental parameters for two realizations.

	Power (mW)	$\Omega_z$ ( $2\pi \times$ kHz)	$\hbar\Omega_z/k_B$ ( $\mu$ K)
NP1	168	200	9.6
NP2	295	256	12

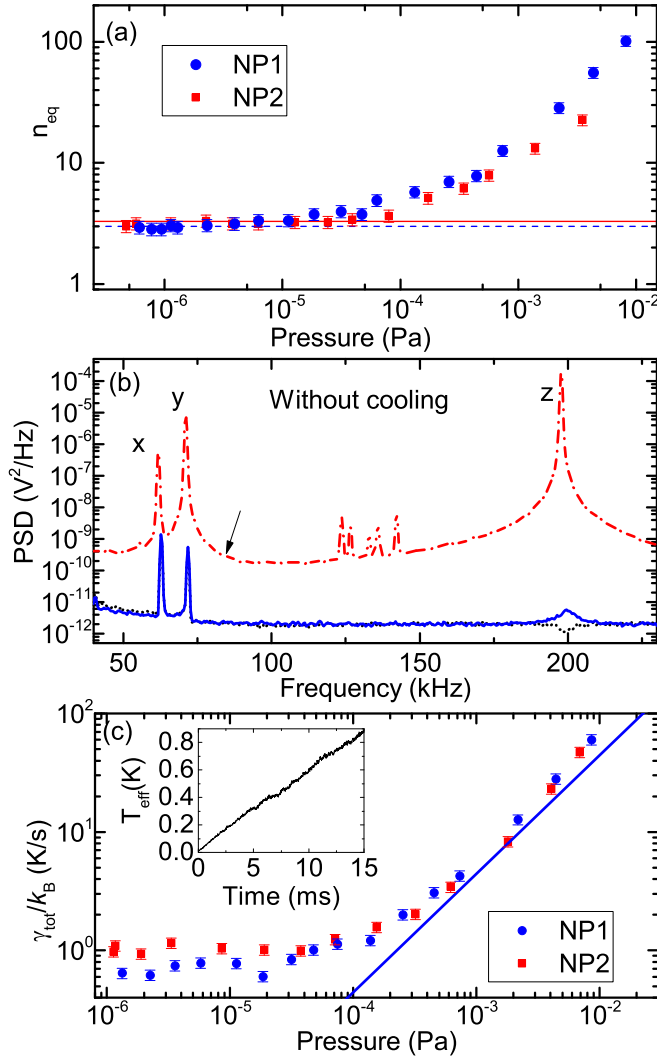


FIG. 2. (a) Occupation number along the optical lattice as a function of the pressure for two experimental realizations (Table I). The gain for feedback cooling is optimized at each pressure. Error bars indicate typical thermal fluctuations in determining  $T_{\text{eff}}$  [33]. Theoretically expected values of  $n_{\text{eq}}$  at low pressures, given by Eq. (6), are shown by blue dashed and red solid lines for NP1 and NP2, respectively. (b) PSDs of the motion of trapped nanoparticles (NP1) with (the black dotted and the blue solid curves for the IL and OL signals, respectively, at  $1.3 \times 10^{-6}$  Pa and without feedback cooling (the red dot-dashed curve, the OL signal at 9.9 Pa). (c) Heating rate as a function of the pressure for two experimental realizations. The vertical errors indicate typical thermal fluctuations. A solid line shows calculated values for NP1 with the kinetic theory [18,19,32]. In the inset, a typical time evolution of  $T_{\text{eff}}$  in the absence of feedback cooling is shown, where the signal is averaged over 256 times. At low pressures, the heating rate is dominated by the photon recoil heating.

When the pressure is decreased to below  $1 \times 10^{-5}$  Pa, under the condition that the LPN is minimized, the occupation number along the optical lattice,  $n_{\text{eq}} = T_{\text{eff}}/\hbar\Omega_z - 1/2$ , is nearly independent from the pressure and approaches the minimum value of about 3, suggesting that the influence of background gases becomes negligible at this pressure region

[Figs. 2(a) and 2(b)]. This fact is further confirmed by measuring the magnitude of the heating via observing the time evolution of the amplitude of the oscillation signal from the OL detector [18,19]. The measured heating rate as a function of the pressure [Fig. 2(c)] is in agreement with the kinetic theory at high pressures [16–18], while it is nearly independent from the pressure at pressures lower than  $1 \times 10^{-5}$  Pa. The heating rate observed in this pressure region is about  $k_B \times 1$  K/s, where  $k_B$  is the Boltzmann constant, in agreement with previous studies on photon recoil heating [32]. In what follows, we work at this pressure region to reveal to what extent the LPN and the photon recoils contribute to the observed heating rate for two individual experimental realizations with different laser powers (Table I).

The magnitude of the heating via the LPN increases with the distance between the trap position and the retroreflecting mirror [Fig. 1(b)]. In our previous setup with the retroreflecting mirror placed outside the vacuum chamber [18], we observed that  $T_{\text{eff}}$  along the optical lattice was limited to a few millikelvins. We found that the LPN of the fiber laser was the source of heating and improved our setup such that the retroreflecting mirror is placed at a distance of  $d = 14.5$  mm from the trap position, which is more than 1 order of magnitude shorter than that of typical experiments with optical lattices and our previous work [18,33]. Furthermore, we decrease the LPN itself by several orders of magnitude via stabilizing the frequency of the laser with a high-finesse resonator. In our setup, we are able to tune the LPN by controlling the feedback gain for the frequency stabilization on the feedback circuit. We estimate the PSD of the LPN by multiplying  $\alpha^2$  by the PSD of the error signal from the resonator, with  $\alpha$  being the slope of the error signal near the resonance. Figure 3(a) shows the PSD of the LPN for three values of the feedback gain  $G$ . Among the three gain values, we observe a dramatic variation in  $T_{\text{eff}}$  [Fig. 3(b)].  $T_{\text{eff}}$  is the lowest at the highest gain with  $G = 0.97$  as expected, while we observe the highest  $T_{\text{eff}}$  among the three at the medium gain with  $G = 0.13$ . In Fig. 3(a), we clearly observe that the LPN near the oscillation frequency is the largest at  $G = 0.13$ . Thus, qualitatively we find that the LPN near  $\Omega_z$  has a dominant contribution to the observed heating, in agreement with our theoretical model.

For further quantitative analysis, we derive the calculated values of  $\gamma_p$  according to Eq. (5) and compare them with the measured values of  $\gamma_{\text{tot}}$  [Fig. 4(a)]. For two experimental realizations, we find a good agreement between measurements and calculations. The linear fits on the plots give slopes of 0.96(12) and 0.99(7) for NP1 and NP2, respectively, which are close to the expected value of unity and suggest that the measured increases in  $\gamma_{\text{tot}}$  are in fact due to the increase in the LPN. The intercepts obtained from the fits are  $k_B \times 0.51(7)$  and  $k_B \times 0.79(7)$  K/s for NP1 and NP2, respectively. These values are also in agreement with our calculation on  $\gamma_r$  providing the values of  $k_B \times 0.46$  and  $k_B \times 0.76$  K/s for NP1 and NP2, respectively [33]. These agreements imply that the approximation of Eq. (3) is valid and nanoparticles are heated dominantly by the LPN near their oscillation frequency. Furthermore, we find that  $n_{\text{eq}}$  observed as a function of the measured values of  $\gamma_{\text{tot}}$  [Fig. 4(b)] is in good agreement with Eq. (6). In Fig. 4(a), we clearly observe that, when the LPN

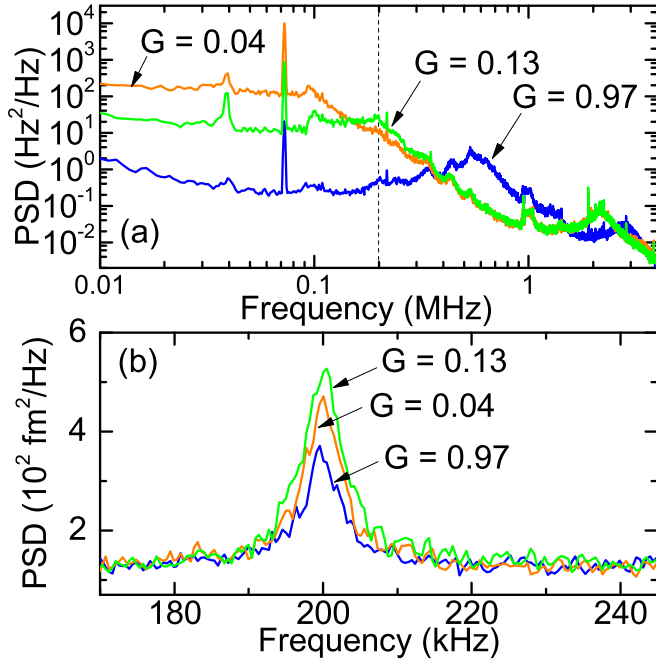


FIG. 3. (a) PSDs of the LPN for three gain values.  $G$  designates the proportional gain values of the proportional-integral regulator for stabilizing the laser frequency. For  $G = 0.97$ , the LPN below 300 kHz is minimized and we achieve recoil-limited feedback cooling as shown in Fig. 2(a). The oscillation frequency for NP1 is shown by a dashed line. The peaks below 100 kHz are due to the bandwidth of the fiber laser itself. (b) PSDs of the OL signal of NP1 for the three profiles of panel (a). The pressure is  $1.3 \times 10^{-6}$  Pa.

is minimized,  $\gamma_{\text{tot}}$  approaches the values determined solely by photon recoil heating, indicating that the impact of the LPN is made negligible in our system. Thus, we can safely claim that the lowest  $n_{\text{eq}}$  value obtained in the present study is limited purely by photon recoil heating.

*Discussions.* The impact of the LPN in the presence of a standing wave potential has been of great concern in recent studies on cavity cooling nanoparticles in a single-beam optical trap. A standing wave potential in an optical resonator shaken by the LPN has a significant heating effect [24], where the occupation number is limited to about  $2 \times 10^3$ . Another recent work in the same direction has shown that nanoparticles are cooled to their ground state when they are placed at the intensity *minimum* of the standing wave potential and are supported by another laser trap [25], as opposed to our situation where nanoparticles are levitated by an optical lattice alone and stay at the intensity *maximum*. Our study offers a distinct approach for circumventing the strong heating issue associated with a standing wave potential.

For the use of our system in future quantum mechanical experiments, the occupation number of  $n_{\text{eq}} < 1$  is preferred. It has been shown that  $S_n$  is inversely proportional to the efficiency of collecting the light scattered by nanoparticles  $\eta$  [37,38]. In our current setup, we estimate that  $\eta$  can be increased by about a factor of 6 via improving the optical and electronic setups, implying that reaching a mean occupation number of  $n_{\text{eq}} < 1$  with a high probability in  $n = 0$  is feasible without the necessity of introducing an optical

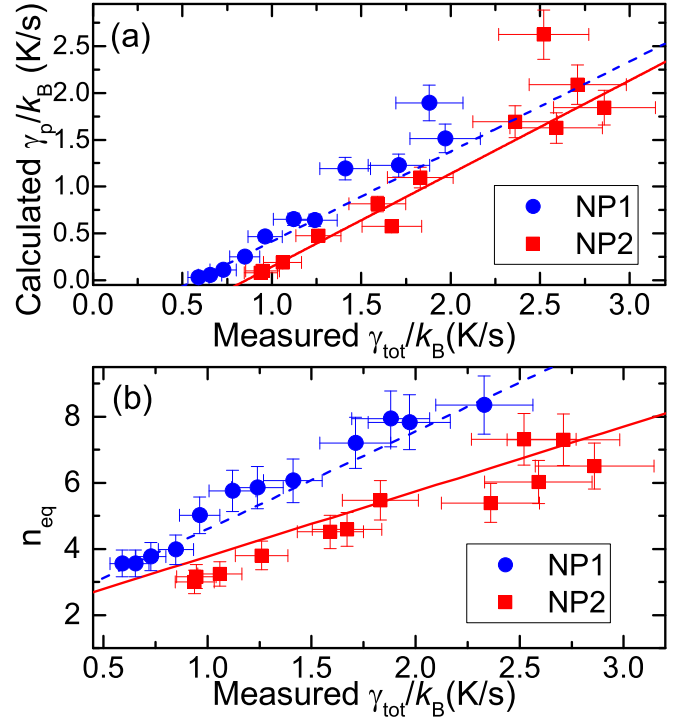


FIG. 4. (a) Comparison between the calculated values of  $\gamma_p$  and the measured values of  $\gamma_{\text{tot}}$  at  $1.3 \times 10^{-6}$  Pa. The horizontal and vertical error bars are due to systematic errors in thermal fluctuations and the error in determining  $\alpha$ , respectively. The blue dashed line and the red solid line are linear fits on the data points for NP1 and NP2, respectively. (b)  $n_{\text{eq}}$  as a function of the measured  $\gamma_{\text{tot}}$  at  $1.3 \times 10^{-6}$  Pa.  $n_{\text{eq}}$  is measured by varying the feedback gain for stabilizing the laser frequency while  $\Gamma_c$  is kept constant. The horizontal and vertical error bars indicate typical thermal fluctuations. The blue dashed line and the red solid line show calculations with Eq. (6) with measured values of  $\Gamma_c$  for NP1 and NP2, respectively, and are not fits.

resonator for cavity sideband cooling [25]. Enhancing the detection sensitivity is important not only for cooling but also for future intriguing physics, where the capability of detecting the zero-point motion of single nanoparticles may allow the direct observation and manipulation of their quantum behaviors. We also note that the position sensitivity of  $1.0 \times 10^{-28}$  m<sup>2</sup>/Hz achieved in the present work [Fig. 3(b)] is orders of magnitude higher than previous studies [26,39] and suggests an application of our system in sensitive accelerometers.

*Conclusions.* In summary, we demonstrate direct feedback cooling of single nanoparticles in an optical lattice to near their ground state in high vacuum. Both the occupation number and the heating rate along the optical lattice are reduced as the LPN is decreased, in good agreement with calculations based on a model taking into account the effect of the LPN. Under the minimum LPN in our setup, the occupation number is limited purely by photon recoil heating. Our results show that the reduction of the LPN near the oscillation frequency of nanoparticles is crucial for working with them near the ground state. Although photon recoil heating is an unavoidable issue with optical levitation, the occupation number can be further reduced by improving the optical setup. Once cooled

to the ground state, our system will provide an important testbed for investigating the quantum superposition states of macroscopic objects [11,12] with masses of the order of 0.1 pg. In comparison with recent other approaches [25,26], our system possesses a qualitatively different control knob for manipulating the position of nanoparticles and for modulating the optical potential via the laser frequency, opening up the possibility to explore the physics with a time-dependent optical lattice [40–42] and anharmonic potentials [43,44] at a single-particle level.

*Acknowledgments.* We thank M. Kozuma for fruitful discussions. We are grateful to T. Naruki for his experimental assistance at the early stage of the experiments. This work is supported by the Murata Science Foundation, the Mitsubishi Foundation, the Challenging Research Award, the “Planting Seeds for Research” program, a STAR Grant funded by the Tokyo Tech Fund, the Research Foundation for Opto-Science and Technology, JSPS KAKENHI (Grants No. JP16K13857, No. JP16H06016, and No. JP19H01822), and JST PRESTO (Grant No. JPMJPR1661).

- 
- [1] A. Derevianko and H. Katori, *Rev. Mod. Phys.* **83**, 331 (2011).
- [2] A. D. Ludlow, M. M. Boyd, J. Ye, E. Peik, and P. O. Schmidt, *Rev. Mod. Phys.* **87**, 637 (2015).
- [3] M. S. Safronova, D. Budker, D. DeMille, D. F. J. Kimball, A. Derevianko, and C. W. Clark, *Rev. Mod. Phys.* **90**, 025008 (2018).
- [4] H. Häffner, C. F. Roos, and R. Blatt, *Phys. Rep.* **469**, 155 (2008).
- [5] M. Saffman, T. G. Walker, and K. Mølmer, *Rev. Mod. Phys.* **82**, 2313 (2010).
- [6] I. Bloch, J. Dalibard, and W. Zwerger, *Rev. Mod. Phys.* **80**, 885 (2008).
- [7] J. Dalibard, F. Gerbier, G. Juzeliūnas, and P. Öhberg, *Rev. Mod. Phys.* **83**, 1523 (2011).
- [8] G. Ranjit, M. Cunningham, K. Casey, and A. A. Geraci, *Phys. Rev. A* **93**, 053801 (2016).
- [9] D. Hempston, J. Vovrosh, M. Toroš, G. Winstone, M. Rashid, and H. Ulbricht, *Appl. Phys. Lett.* **111**, 133111 (2017).
- [10] E. Hebestreit, M. Frimmer, R. Reimann, and L. Novotny, *Phys. Rev. Lett.* **121**, 063602 (2018).
- [11] O. Romero-Isart, A. C. Pflanzer, F. Blaser, R. Kaltenbaek, N. Kiesel, M. Aspelmeyer, and J. I. Cirac, *Phys. Rev. Lett.* **107**, 020405 (2011).
- [12] A. Bassi, K. Lochan, S. Satin, T. P. Singh, and H. Ulbricht, *Rev. Mod. Phys.* **85**, 471 (2013).
- [13] A. Arvanitaki and A. A. Geraci, *Phys. Rev. Lett.* **110**, 071105 (2013).
- [14] A. A. Geraci, S. B. Papp, and J. Kitching, *Phys. Rev. Lett.* **105**, 101101 (2010).
- [15] T. Li, S. Kheifets, and M. G. Raizen, *Nat. Phys.* **7**, 527 (2011).
- [16] J. Gieseler, B. Deutsch, R. Quidant, and L. Novotny, *Phys. Rev. Lett.* **109**, 103603 (2012).
- [17] J. Vovrosh, M. Rashid, D. Hempston, J. Bateman, M. Paternostro, and H. Ulbricht, *J. Opt. Soc. Am. B* **34**, 1421 (2017).
- [18] M. Iwasaki, T. Yotsuya, T. Naruki, Y. Matsuda, M. Yoneda, and K. Aikawa, *Phys. Rev. A* **99**, 051401(R) (2019).
- [19] F. Tebbenjohanns, M. Frimmer, A. Militar, V. Jain, and L. Novotny, *Phys. Rev. Lett.* **122**, 223601 (2019).
- [20] G. P. Conangla, F. Ricci, M. T. Cuairan, A. W. Schell, N. Meyer, and R. Quidant, *Phys. Rev. Lett.* **122**, 223602 (2019).
- [21] N. Kiesel, F. Blaser, U. Delić, D. Grass, R. Kaltenbaek, and M. Aspelmeyer, *Proc. Natl. Acad. Sci. U.S.A.* **110**, 14180 (2013).
- [22] P. Asenbaum, S. Kuhn, S. Nimmrichter, U. Sezer, and M. Arndt, *Nat. Commun.* **4**, 2743 (2013).
- [23] J. Millen, P. Z. G. Fonseca, T. Mavrogordatos, T. S. Monteiro, and P. F. Barker, *Phys. Rev. Lett.* **114**, 123602 (2015).
- [24] N. Meyer, A. d. I. Rios Sommer, P. Mestres, J. Gieseler, V. Jain, L. Novotny, and R. Quidant, *Phys. Rev. Lett.* **123**, 153601 (2019).
- [25] U. Delić, M. Reisenbauer, K. Dare, D. Grass, V. Vuletić, N. Kiesel, and M. Aspelmeyer, *Science* **367**, 892 (2020).
- [26] F. Tebbenjohanns, M. Frimmer, V. Jain, D. Windey, and L. Novotny, *Phys. Rev. Lett.* **124**, 013603 (2020).
- [27] M. Yoneda, M. Iwasaki, and K. Aikawa, *Phys. Rev. A* **98**, 053838 (2018).
- [28] P.-F. Cohadon, A. Heidmann, and M. Pinard, *Phys. Rev. Lett.* **83**, 3174 (1999).
- [29] P. Bushev, D. Rotter, A. Wilson, F. Dubin, C. Becher, J. Eschner, R. Blatt, V. Steixner, P. Rabl, and P. Zoller, *Phys. Rev. Lett.* **96**, 043003 (2006).
- [30] M. Poggio, C. L. Degen, H. J. Mamin, and D. Rugar, *Phys. Rev. Lett.* **99**, 017201 (2007).
- [31] D. J. Wilson, V. Sudhir, N. Piro, R. Schilling, A. Ghadimi, and T. J. Kippenberg, *Nature (London)* **524**, 325 (2015).
- [32] V. Jain, J. Gieseler, C. Moritz, C. Dellago, R. Quidant, and L. Novotny, *Phys. Rev. Lett.* **116**, 243601 (2016).
- [33] See Supplemental Material at <http://link.aps.org/supplemental/10.1103/PhysRevA.103.L051701> for the details of experiments and the validity of our model.
- [34] M. Yoneda and K. Aikawa, *J. Phys. B: At., Mol. Opt. Phys.* **50**, 245501 (2017).
- [35] D. S. Bykov, P. Mestres, L. Dania, L. Schmöger, and T. E. Northup, *Appl. Phys. Lett.* **115**, 034101 (2019).
- [36] E. Hebestreit, R. Reimann, M. Frimmer, and L. Novotny, *Phys. Rev. A* **97**, 043803 (2018).
- [37] A. C. Doherty, A. Szorkovszky, G. I. Harris, and W. P. Bowen, *Philos. Trans. R. Soc. A: Math. Phys. Eng. Sci.* **370**, 5338 (2012).
- [38] F. Tebbenjohanns, M. Frimmer, and L. Novotny, *Phys. Rev. A* **100**, 043821 (2019).
- [39] U. Delić, M. Reisenbauer, D. Grass, N. Kiesel, V. Vuletić, and M. Aspelmeyer, *Phys. Rev. Lett.* **122**, 123602 (2019).
- [40] H. Lignier, C. Sias, D. Ciampini, Y. Singh, A. Zenesini, O. Morsch, and E. Arimondo, *Phys. Rev. Lett.* **99**, 220403 (2007).
- [41] P. Hauke, O. Tieleman, A. Celi, C. Ölschläger, J. Simonet, J. Struck, M. Weinberg, P. Windpassinger, K. Sengstock, M. Lewenstein *et al.*, *Phys. Rev. Lett.* **109**, 145301 (2012).
- [42] L.-C. Ha, L. W. Clark, C. V. Parker, B. M. Anderson, and C. Chin, *Phys. Rev. Lett.* **114**, 055301 (2015).
- [43] P. Schmelcher, *Phys. Rev. E* **98**, 022222 (2018).
- [44] A. Dhar, A. Kundu, S. N. Majumdar, S. Sabhapandit, and G. Schehr, *Phys. Rev. E* **99**, 032132 (2019).